Polymer 51 (2010) 2271–2276

Contents lists available at ScienceDirect

Polymer

journal homepage: www.elsevier.com/locate/polymer

# Ethylene slurry polymerization using nickel diimine catalysts covalently-attached onto $MgCl_2$-based supports

Yiyoung Choi, João B.P. Soares*

*Department of Chemical Engineering, University of Waterloo, Ontario, Canada N2L 3G1*

ARTICLE INFO

*Article history:*
Received 12 February 2010
Received in revised form
25 March 2010
Accepted 27 March 2010
Available online 2 April 2010

*Keywords:*
Ethylene polymerization
Nickel diimine catalysts
Supported catalysts

ABSTRACT

$MgCl_2$/alcohol adducts were recrystallized with alkyl aluminums and used as catalysts supports for nickel diimine complexes functionalized with amine groups. These supported catalysts were used to polymerize ethylene in a slurry reactor. The $MgCl_2$-based supported nickel diimine catalysts had higher activities than the equivalent $SiO_2$-supported nickel diimine catalysts, even without the use of activators. These catalysts made polyethylene with melting temperatures and molecular weights higher than those made with the equivalent homogeneous catalysts. Interestingly, the catalyst activity and polymer molecular weight could be controlled by changing the support composition. In addition, covalent chemical bonds between the functionalized nickel diimine complex and the $MgCl_2$-based supports avoided catalyst leaching during polymerization, leading to the production of polymer particles with good morphology. The mechanical strength of the resulting polymer particles, however, was lower than those made with $SiO_2$-supported nickel diimine catalysts.



## 1. Introduction

Olefin polymerization processes in slurry and gas phase reactors require the use of solid-supported catalysts [1,2]. The catalyst should not leach from the support during polymerization, and the catalyst structure, activity, and comonomer reactivity must be maintained after supporting. Presently, the most common type of support for heterogeneous Ziegler–Natta catalysts is $MgCl_2$. These industrial catalysts are extremely active and produce polymer particles with high density and excellent morphology.

Several researchers showed that $MgCl_2$ could also be used as an effective support for early and late transition metal single-site catalysts. Xu et al. supported Fe(II) and Ni(II) catalysts onto spherical $MgCl_2$ particles by direct impregnation. The activities of the supported catalysts and the properties of the resultant polymers were comparable to those obtained with $SiO_2$-supported catalysts [3]. Nakayama et al. showed that $MgCl_2$-based compounds could act as good activators as well as supports for FI catalysts (bis(phenoxyimine) catalysts). When compared to the corresponding homogeneous system activated with methylaluminoxane (MAO), FI catalysts had higher activity, and made polymer with higher molecular weight averages and controlled particle morphology [4]. Chadwick et al. synthesized $MgCl_2$-based compounds by the recrystallization method, and then used them as supports for various single-site catalysts. They made polyethylene with a spherical particle morphology and small polydispersity index (PDI) [5,6].

Although the catalysts activities reported using physisorbed $SiO_2$-supported nickel diimine catalysts were very low and produced polymer with poor morphology [7,8], $SiO_2$-supported nickel diimine catalysts where the catalyst sites had been covalently bonded to the support were very active, did not leach appreciably from the surface, and did not cause reactor fouling [8–10].

In this work, $MgCl_2$/alcohol adducts were crystallized using several alkyl aluminums and used as supports for nickel diimine complexes functionalized with amine groups. We propose that the catalysts were covalently bonded to the support surface through their amine functionalities, leading to high ethylene polymerization activity and the production of polymer powders with good morphologies. The polymer properties were controlled by varying the polymerization conditions, the structure of the nickel diimine complexes, and the chemical components of the support. The microstructures of the resultant polymers were analyzed by several techniques and the morphologies of the polymer particles were characterized by scanning electron microscope (SEM).

## 2. Experimental

### 2.1. Materials

All operations were performed under nitrogen (99.999%, from Praxair) using standard Schlenk techniques or inside a glove-box

* Corresponding author. Fax: +1 519 746 4979.
*E-mail address:* jsoares@uwaterloo.ca (J.B.P. Soares).

0032-3861/$ – see front matter Crown Copyright © 2010 Published by Elsevier Ltd. All rights reserved.
doi:10.1016/j.polymer.2010.03.051

(Vacuum Atmosphere Company, Nexus). Polymer grade ethylene (99.9%, from Praxair) and nitrogen were purified by passing through columns packed with R3-11 copper catalyst, activated alumina and 3A/4A mixed molecular sieves. Materials for nickel diimine complex synthesis, anhydrous $MgCl_2$, methanol (99.8%), isopropyl alcohol (99.5%) and 2-ethyl hexanol (99.6%) were purchased from Aldrich and used without further purification. Trimethyl aluminum (TMA, 2 M in hexane), and triisobutyl aluminum (TIBA, 1 M in hexane) were purchased from Aldrich. Ethyl aluminum sesquichloride (EASC, 97%) was kindly donated by Akzo Nobel. Solvents for catalyst synthesis and polymerization were purified by passing through columns packed with molecular sieves (Zeolum Type F-9, Tosoh Co.). All purified solvents were stored in Schlenk flasks with 3A/4A mixed molecular sieves.

### 2.2. Synthesis of nickel diimine complexes

The syntheses of nickel diimine complexes followed procedures published in the literature and will be briefly described below [8,10].

#### 2.2.1. Bis(4-amino-2,3,5,6-tetramethylimino)acenaphtene nickel(II) dibromide (*N1*)

An amount of 8.2 mmol acenaphtenequinone, 30.0 mmol 2,3,5,6,-tetramethyl-phenylene-1,4-diamine, and 50 mL toluene as solvent were added to a 100 mL Schlenk flask. A volume of 0.03 mL sulfuric acid as reaction catalyst was added dropwise to the flask. The mixture was stirred and refluxed for 3 h. After the insoluble residue was filtered while still hot, the product was dried under vacuum. The dried powder was dissolved in 200 mL ethyl acetate, 400 mL hexane was added, and the mixture was stirred for 30 min. This solution was kept in the freezer at −15 °C overnight. The precipitated product was filtered and washed with 50 mL cold hexane, and vacuum-dried overnight. A dried red powder (2.75 g, 71% yield) was obtained.

An amount of 1.6 mmol nickel(II) dibromide-ethyleneglycol dimethylether complex ($NiBr_2$(DME)) and 1.8 mmol bis(4-amino-2,3,5,6-tetramethylimino)acenaphtene were added to a 50 mL Schlenk flask, then dissolved with 20 mL dichloromethane. After the mixture was stirred for 3 days at room temperature, dichloromethane was removed by vacuum. The product was washed three times with 20 mL diethyl ether each time, and then dried under vacuum. A dried black powder (0.8 g, 73% yield) was isolated and named **N1**.

(Elemental Analysis result (**N1**, $C_{32}H_{34}N_4Br_2Ni$) (695.6): Calculated: C 55.3, H 5.3, N 8.1; Found: C 55.0, H 5.2, N 8.0).

#### 2.2.2. Bis(4-amino-2,3,5,6-tetramethylimino)butane nickel(II) dibromide (*N2*)

An amount of 10 mmol 2,3 butanedione, 30.0 mmol 2,3,5,6,-tetramethyl-phenylene-1,4-diamine, and 50 mL benzene as solvent were added to a 100 mL Schlenk flask. A volume of 0.03 mL sulfuric acid as reaction catalyst was added dropwise to the flask. The mixture was stirred and refluxed for 3 h. The insoluble residue was removed by filtration while still hot and dried overnight under vacuum. A volume of 200 mL cold hexane was added to the flask containing the dried product and stirred for 2 h. The solid fraction was filtered and washed with 100 mL cold hexane, and vacuum dried overnight. A dried yellow powder (2.90 g, 77% yield) was obtained.

An amount of 1.6 mmol nickel(II) dibromide-ethyleneglycol dimethylether complex ($NiBr_2$(DME)) and 1.8 mmol bis(4-amino-2,3,5,6-tetramethylimino)butane were added to a 50 mL Schlenk flask, then dissolved with 20 mL dichloromethane. After the mixture was stirred for 3 days at room temperature, dichloromethane was removed by vacuum. The product was washed three times with 20 mL diethyl ether each time, and then dried under vacuum. A dried brown powder (0.7 g, 67% yield) was isolated and named **N2**.

(Elemental Analysis result (**N2**, $C_{24}H_{34}N_4Br_2Ni$) (599.5): Calculated: C 48.1, H 6.1, N 9.3; Found: C 47.8, H 6.2, N 9.6).

Fig. 1 shows the chemical structures of the **N1** and **N2** catalysts.

### 2.3. Synthesis of $MgCl_2$-based supported nickel diimine catalysts

An amount of 10 mmol of anhydrous $MgCl_2$, 30 mmol 2-ethyl hexanol, and 25 mL hexane were added to a dried 225 mL glass reactor equipped with a mechanical stirrer (Lab-Crest Glass Pressure Reaction Vessels, Andrews Glass Co.). After the mixture was maintained at 100 °C overnight and cooled to room temperature, a clear $MgCl_2$/alcohol adduct solution was obtained. An amount of 50 mmol TMA was added dropwised into the solution under 100 rpm. When 10% of TMA was added, the $MgCl_2$/alcohol adduct begun to crystallize. After complete addition of the TMA for 1 h, the mixture was allowed to react for 4 more hours. The stirring was stopped, the supernatant liquid was removed with a cannula, and the solid product was washed two times with 20 mL dichloromethane. An amount of 0.08 mmol **N1** was dissolved in 20 mL dichloromethane, added the precipitated solid, and allowed to react for 15 h. After the catalyst particles were precipitated, the black color of **N1** solution disappeared, and a transparent solvent phase was separated. This indicates that **N1** was almost completely supported onto the $MgCl_2$-based support. The supported catalyst was filtered, washed with 20 mL dichloromethane, and then dried under vacuum. This supported catalyst was named $MgCl_2$-based supported **N1** catalyst (**N1Mg**). $MgCl_2$-based supported **N2** catalyst (**N2Mg**) was synthesized according to same procedure using **N2**. Table 1 lists the chemical components of all supported catalysts made with this procedure.

The **N1** catalyst was also supported on $SiO_2$ to serve as a reference for comparison with the $SiO_2$-supported catalysts. One gram of silica (Grace Davison, XPO 2410) and 20 mL toluene were introduced in a same glass reactor. The reactor was heated to 60 °C

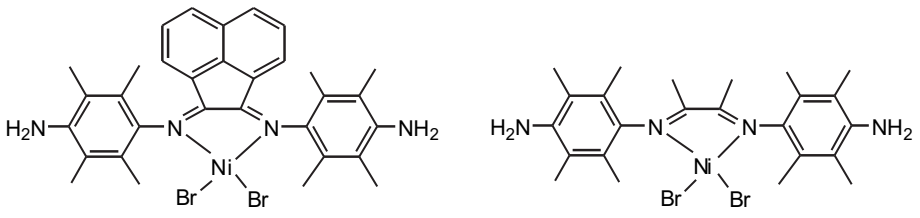


N1 N2

**Fig. 1.** Structures of nickel diimine complexes: bis(4-amino-2,3,5,6-tetramethylimino)acenaphtene nickel(II) dibromide (**N1**) and bis(4-amino-2,3,5,6-tetramethylimino)butane nickel(II) dibromide (**N2**).

**Table 1**
Description of prepared $MgCl_2$-based supported nickel diimine catalysts.

| Entry | Used Chemical Components | | | | Characterization Results | | | | | Supporting Efficiency[a] | | | |
|---|---|---|---|---|---|---|---|---|---|---|---|---|---|
| | Ni complex (mmol) | $MgCl_2$ (mmol) | Alcohol (mmol) | Alkyl aluminum (mmol) | Ni (mmol/g catalyst) | Mg (mmol/g catalyst) | Cl (mmol/g catalyst) | O (mmol/g catalyst) | Al (mmol/g catalyst) | Mg (wt.-%) | Cl (wt.-%) | O (wt.-%) | Al (wt.-%) |
| 1 | N1 0.08 | 10 | 2-Ethyl hexanol 30 | TMA 50 | 0.053 | 6.21 | 8.61 | 17.59 | 0.85 | 93.7 | 65.0 | 88.5 | 2.6 |
| 2 | N1 0.08 | 10 | 2-Ethyl hexanol 30 | TIBA 50 | 0.049 | 5.09 | 6.91 | 16.23 | 1.11 | 83.1 | 56.4 | 88.3 | 3.6 |
| 3 | N1 0.08 | 10 | Methanol 30 | TMA 50 | 0.053 | 6.05 | 8.44 | 17.88 | 1.04 | 90.9 | 64.0 | 90.0 | 3.2 |
| 4 | N1 0.08 | 10 | Methanol 30 | TIBA 50 | 0.051 | 5.75 | 7.51 | 18.58 | 0.99 | 90.7 | 58.9 | 97.2 | 3.2 |
| 5 | N1 0.08 | 10 | Isopropyl alcohol 30 | TMA 50 | 0.049 | 5.76 | 9.60 | 19.81 | 0.73 | 94.2 | 78.4 | 92.6 | 2.4 |
| 6 | N2 0.08 | 10 | 2-Ethyl hexanol 30 | TMA 50 | 0.055 | 6.14 | 7.74 | 16.89 | 0.82 | 91.4 | 56.2 | 81.9 | 2.4 |

[a] Calculated by assuming 100% Ni deposition for the supported chemical components.

at a stirring rate of 100 rpm, then 20 mmol TMA was slowly added and reacted for 15 h. After stopping the stirrer, the supernatant liquid was removed with a cannula, the product was washed two times with 20 mL toluene. An amount of 0.08 mmol **N1** was added to the product with 20 mL dichloromethane, and allowed to react for 15 h under 100 rpm at room temperature. The produced supported catalyst (**N1Si**) was filtered and washed with 20 mL dichloromethane, and dried under vacuum. The analyzed Ni content was 0.65 wt.-%.

### 2.4. Characterization of supported nickel diimine catalysts

Ni, Al and Mg contents on the supported catalysts were measured by inductively coupled plasma-optical emission spectroscopy (ICP, Teledyne Leeman Labs, Prodigy High Dispersion ICP). A mass of 20 mg of supported catalyst was dissolved in 10 mL 3 N $HNO_3$ solution. The solution was diluted with distilled water prior to analysis. A LEO 1530 scanning electron microscope (SEM) combined energy dispersive X-ray (EDX) analysis was used to investigate the morphology of the catalysts and organic elements of the supported catalysts. For the SEM/EDX analysis, the supported catalysts particles were embedded onto an epoxy resin and cut into slices of 120 nm thicknesses with a diamond knife.

### 2.5. Polymerization

Polymerizations were carried out in a 300 mL semi-batch autoclave, equipped with a mass flow controller and a temperature control unit consisting of a cooling coil and an electric heater. The polymerization temperature was maintained within ±0.2 °C of the set point. Prior to each reaction, the reactor was purged several times with nitrogen, then heated to 120 °C under vacuum and purged again to the set point temperature under nitrogen flow. A volume of 150 mL hexane and 1 mmol EASC or 0.1 mmol TIBA was transferred to the reactor. After introducing the supported catalyst in hexane slurry, polymerization took place under a continuous ethylene flow to meet the desired pressure. At the end of the polymerization time, the reactor was rapidly vented and the resultant polymer was precipitated and washed with acidified ethanol, then filtered and dried under vacuum.

### 2.6. Polymer characterization

The catalyst activity was calculated as the mass of polymer product divided by mmol catalyst per hour. The melting temperature ($T_m$) of the resultant polymer was characterized using differential scanning calorimetry (DSC, TA Instruments Q2000). The second scan was done at a heating rate of 10 °C/min and used to characterize the sample. The polymer molecular weight distribution was determined by gel permeation chromatography (GPC, Polymer Char). Samples were dissolved at 145 °C with 1,2,4-trichlorobenzene and passed through three linear Polymer Laboratories columns which were calibrated with polystyrene standards and operated with a flow rate of 1 mL/min. Short chain branching distributions (SCBD) were determined by crystallization analysis fractionation (CRYSTAF, Polymer Char). Samples were dissolved at 160 °C for 30 min followed by 60 min of equilibration at 95 °C. The cooling rate during crystallization was 0.1 °C/min, from 95 °C to 30 °C. A SEM was used to investigate the morphology of polymer particles.

## 3. Results and discussion

### 3.1. Structure of $MgCl_2$-based supported nickel diimine catalysts

Fig. 2 describes the preparation steps for the synthesis of **N1Mg**. The reaction of TMA with $MgCl_2$/methanol adduct in hexane diluent leads to the precipitation of the $MgCl_2$-based support. The **N1** complex is likely supported through one or two of its amine functional groups, creating covalent bonds with the $MgCl_2$-based support.

Fig. 3 shows a SEM image of a spherical catalyst particle containing several wide cracks. These cracks may be formed when the epoxy-embedded particle was microtomed with the diamond knife, and indicates that its mechanical strength is not very high.

Table 1 lists the chemical components and characterization results for $MgCl_2$-based supported catalysts investigated in this

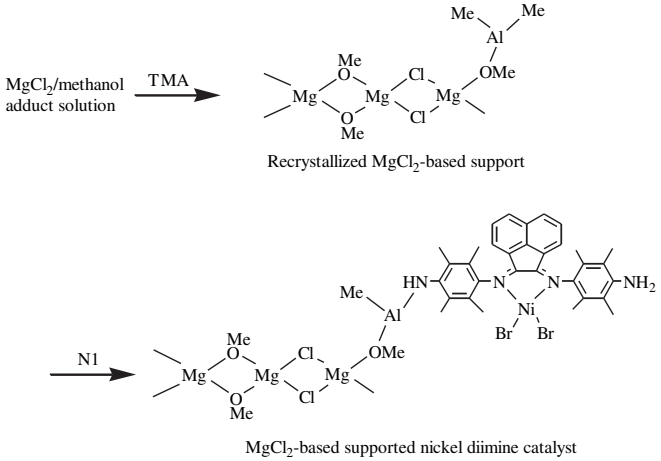


**Fig. 2.** Preparation of $MgCl_2$-based supported nickel diimine catalyst (**N1Mg**).

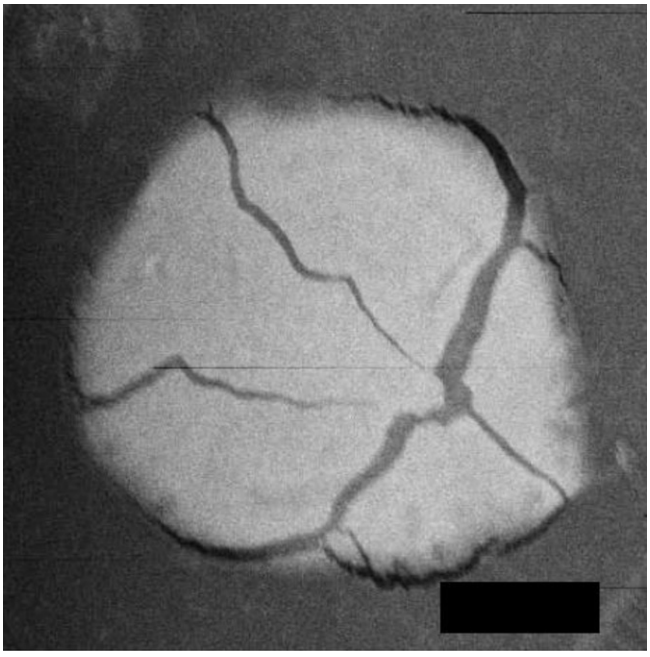

**Fig. 3.** SEM micrograph of a **N1Mg** particle (Entry 1 in the Table 1, scale bar 5 μm).

study. Compared with the content of other elements, the fraction of Al on the support is relatively low. It seems that the alkyl aluminum acts mostly as a dealcoholation reagent, helping crystallize the $MgCl_2$/alcohol adducts, and that only a small fraction of the alkyl aluminum molecules become chemically-bonded onto the $MgCl_2$-based support surface. It is also possible that excess alkyl aluminum molecules are removed during the catalyst washing steps.

### 3.2. Ethylene polymerization

Ethylene polymerizations using homogeneous and $SiO_2$-supported nickel diimine catalysts were conducted to serve as a reference for the polymerizations using $MgCl_2$-based supported nickel diimine catalysts. Table 2 summarizes these polymerization results. In general, a significant reduction on catalyst activity is observed when homogeneous catalysts are supported on several different carriers. This behavior has been attributed to catalyst poisoning by functional groups and impurities present on the catalyst surface, or to steric hindrance caused by the support [11]. In the present investigation, however, the activities of the supported catalysts were comparable to those of the homogeneous catalysts. It seems that the **N1** and **N2** complexes are covalently bonded to the support through their amine groups, forming highly active and strongly immobilized metal centers [8–10,12]. The homogeneous **N1** catalyst was more active, and produced polymer with lower $T_m$, than the homogeneous **N2** catalyst; these trends were the same when **N1** and **N2** were supported on $SiO_2$ or $MgCl_2$-based supports.

Interestingly, the **N1Mg** had higher activity than **N1Si** (Runs 3 and 5, Table 2), and its activity was nearly 90% of the homogeneous catalysts (Runs 1 and 5, Table 2). The activity of **N2Mg** was even slightly higher than that of the homogeneous **N2** complex (Runs 2 and 7, Table 2). Both **N1Mg** and **N2Mg** also had considerable high activities in the absence of the EASC activator. The Lewis acidic $MgCl_2$-based supports may be able to activate nickel diimine complexes, as reported by Marks et al. [13]. The melting temperature ($T_m$) and weight average molecular weight ($M_w$) of the polymer made with the supported catalysts without activator were also a little higher than those made in the presence of the EASC, indicating that EASC favored β-hydride elimination and chain walking.

Comparative CRYSTAF results are shown in Fig. 4. Polyethylenes made with **N1Mg** and **N1** had different microstructures. The polymer made with **N1** (Run 1, Table 2) had a broader

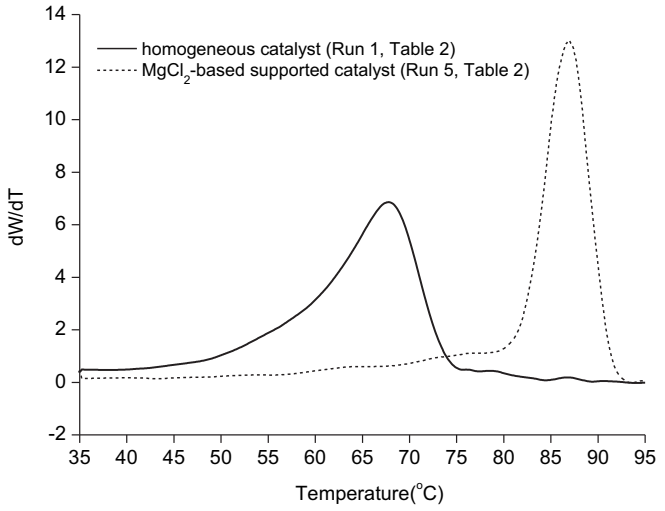


**Fig. 4.** Crystaf (SCBD) profiles of polyethylene made with **N1** and **N1Mg**.

**Table 2**
Comparison of ethylene polymerization results with homogeneous and supported nickel diimine catalysts.

| Run | Polymerization Conditions | | Results | | | |
|---|---|---|---|---|---|---|
| | Catalyst | Activator | Activity[a] | $M_w$ (g/mol × $10^{-3}$) | *PDI*[b] | $T_m$ (°C) |
| 1 | N1 | EASC | 41 200 | 60 | 2.8 | 115.2 |
| 2 | N2 | EASC | 6900 | 67 | 3.3 | 122.8 |
| 3 | N1Si | EASC | 29 600 | 143 | 5.8 | 126.7 |
| 4 | N1Si | Not used | 1460 | 167 | 4.9 | 127.1 |
| 5 | N1Mg | EASC | 36 450 | 127 | 5.5 | 125.5 |
| 6 | N1Mg | Not used | 12 550 | 140 | 5.5 | 126.6 |
| 7 | N2Mg | EASC | 7250 | 154 | 5.8 | 123.5 |
| 8 | N2Mg | Not used | 4960 | 172 | 5.9 | 124.4 |

Polymerization conditions: homogeneous catalyst 0.5 μmol, supported catalyst 10–20 mg, EASC 1 mmol, TIBA 0.1 mmol in Runs 4, 6, 8; solvent 150 mL hexane, ethylene pressure 150 psig, temperature 60 °C, time 15 min; $MgCl_2$-based support: $MgCl_2$/2-ethyl hexanol/TMA.
[a] Activity in kg PE/(mol Ni × h).
[b] Polydispersity index ($M_w/M_n$).

**Table 3**
Ethylene polymerization results using MgCl2-based supported nickel diimine catalysts in the absence of activator.

| Run | Polymerization Conditions | | | Results | | | |
|---|---|---|---|---|---|---|---|
| | Catalyst | Pressure (psig) | Temperature (°C) | Activity[a] | $M_w$ (g/mol × $10^{-3}$) | *PDI*[b] | $T_m$ (°C) |
| 1 | N1Mg | 150 | 30 | 4590 | 202 | 4.4 | 129.6 |
| 2 | N1Mg | 150 | 60 | 12 550 | 140 | 5.5 | 126.6 |
| 3 | N1Mg | 150 | 80 | 7690 | 84 | 5.3 | 124.1 |
| 4 | N1Mg | 50 | 60 | 4400 | 110 | 5.3 | 123.8 |
| 5 | N2Mg | 150 | 30 | 3620 | 334 | 5.2 | 129.0 |
| 6 | N2Mg | 150 | 60 | 4960 | 172 | 5.9 | 124.4 |
| 7 | N2Mg | 50 | 30 | 1470 | 211 | 5.8 | 126.4 |

Polymerization conditions: catalyst 30–40 mg, TIBA 0.1 mmol, solvent 150 mL hexane, time 15 min.
$MgCl_2$-based support: $MgCl_2$/2-ethyl hexanol/TMA.
[a] Activity in kg PE/(mol Ni × h).
[b] Polydispersity index ($M_w/M_n$).

**Table 4**
Effect of the support components using **N1** complex on ethylene polymerization.

| Run | Conditions | | | Results | | | |
|---|---|---|---|---|---|---|---|
| | $MgCl_2$-based supports | | Temperature (°C) | Activity[a] | $M_w$ (g/mol × $10^{-3}$) | *PDI*[b] | $T_m$ (°C) |
| | Alcohol | Alkyl Aluminum | | | | | |
| 1 | 2-Ethyl hexanol | TMA | 30 | 7590 | 204 | 5.4 | 129.6 |
| 2 | 2-Ethyl hexanol | TIBA | 30 | 7290 | 273 | 5.8 | 130.8 |
| 3 | Methanol | TMA | 30 | 12 890 | 199 | 5.6 | 131.1 |
| 4 | Methanol | TIBA | 30 | 8970 | 213 | 5.1 | 129.7 |
| 5 | Isopropyl alcohol | TMA | 30 | 8300 | 198 | 5.3 | 129.9 |
| 6 | 2-ethyl hexanol | TMA | 60 | 12 550 | 140 | 5.5 | 126.5 |
| 7 | 2-Ethyl hexanol | TIBA | 60 | 11 080 | 154 | 6.3 | 128.0 |
| 8 | Methanol | TMA | 60 | 18 200 | 144 | 6.4 | 128.2 |
| 9 | Methanol | TIBA | 60 | 14 290 | 152 | 5.7 | 126.9 |
| 10 | Isopropyl alcohol | TMA | 60 | 13 150 | 145 | 5.6 | 127.0 |

Polymerization conditions: catalyst 30–40 mg, TIBA 0.1 mmol, solvent 150 mL hexane, time 15 min.
[a] Activity in kg PE/(mol Ni × h).
[b] Polydispersity index ($M_w/M_n$).

SCBD in the temperature range 40–75 °C, while polymer made with **N1Mg** (Run 5, Table 2) had a narrower SCBD (80–90 °C) with a high crystallization temperature peak (>85 °C). It seems that strong steric effects between support and **N1** depress chain walking [14] rates and, therefore, produce polymer chains having lower short chain branch content and higher $T_m$. This is also a clear indication that the catalyst is firmly anchored onto the support surface.

Ethylene polymerization results under different polymerization conditions in the absence of activator are shown in Table 3. As the polymerization temperature increases, a maximum activity is reached at 60 °C, and then decreases for **N1Mg**. On the other hand,

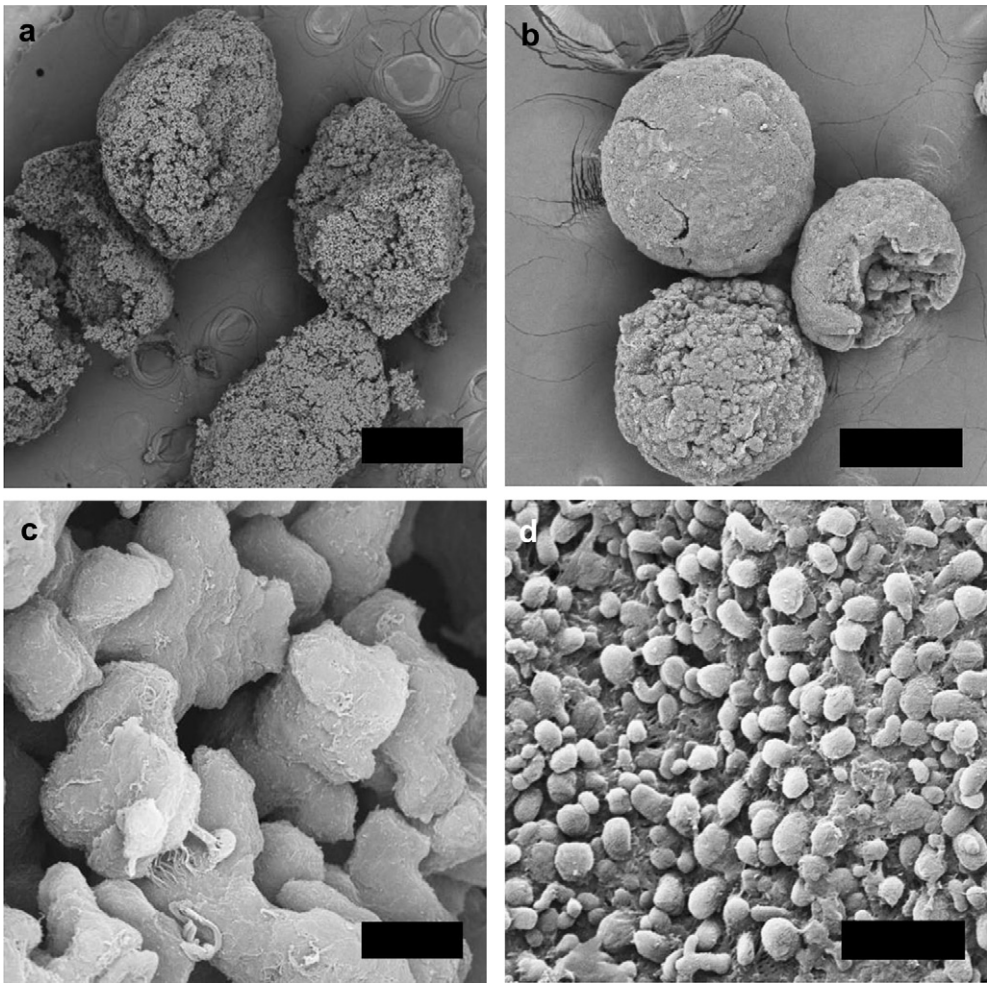


**Fig. 5.** SEM micrographs of polymer particles: a) polyethylene particles using **N1Mg** (Run 5 in Table 2, scale bar 200 μm); b) polyethylene particles made with **N1Si** (Run 3 in Table 2, scale bar 200 μm); c) A closer look at the external surface of a) (scale bar 2 μm); d) A closer look at the external surface of b) (scale bar 2 μm).

the catalyst activity is not very sensitive to temperature variations for **N2Mg**. According to the chain walking mechanism, homogeneous nickel diimine catalysts produce polymers with higher $T_m$ and higher $M_w$ as the ethylene pressure increases or as the polymerization temperature decreases. The $MgCl_2$-based supported nickel diimine catalysts, **N1Mg** and **N2Mg**, obey the same trends observed for homogeneous nickel diimine catalysts.

To compare the effect of support structure on catalyst activity, various alcohols and alkyl aluminums were used to synthesize $MgCl_2$-based supported nickel diimine catalysts; these polymerization results are shown in Table 4. $MgCl_2$-based supports, in combination with methanol/TMA, produced catalysts with the highest activity. It seems that a favorable electronic environment, based on the acidic nature of the support, was generated when methanol/TMA was used. The supported catalyst, in combination with 2-ethyl hexanol/TIBA, made polymer with the highest $M_w$. It is likely that TIBA, with bulky alkyl groups, has a lower chain transfer rate than TMA, and therefore produces polyethylene with higher $M_w$ [15]. Regardless of the support type, the catalysts activities at 60 °C were higher than at 30 °C, but $T_m$ and $M_w$ were lower.

SEM micrographs of the polymer particles made with both $MgCl_2$-based supported catalyst and $SiO_2$-supported catalyst are compared in Fig. 5. There was no reactor fouling during the polymerizations, and free-flowing polymer particles were always obtained. Fig. 5a shows the polymer particles made using **N1Mg** (Run 5, Table 2) had rough and apparently frail surfaces, resulting in particles with irregular shapes and debris. In Fig. 5c, the expanded view of Fig. 5a, the primary particles that compose the larger secondary particles appear as relatively flat stacks with high porosity, which lowers the bulk density of the secondary particles. On the other hand, Fig. 5b depicts polymer particles made with **N1Si** (Run 3, Table 2), where denser and roughly spherical primary and secondary particles (Fig. 5d) are apparent.

## 4. Conclusions

Ethylene slurry polymerizations were performed using various $MgCl_2$-based supported nickel-diimine catalysts. Nickel diimine complexes having amine functional groups were covalently attached onto $MgCl_2$-based supports, producing highly active and strongly immobilized nickel diimine complexes. The Lewis acidic $MgCl_2$-based supports were able to act as activators for the nickel diimine complexes, leading to active polymerization catalysts even in the absence of external alkyl aluminum activators. The chemical structure of the support had an influence on catalyst activity and microstructure of the resultant polymers. The polymers made with $MgCl_2$-based supports resulted in free-flowing particles that did not cause reactor fouling, but were weaker and more porous than the ones made with the equivalent $SiO_2$-supported catalyst.

## References

[1] Mckenna TF, Soares JBP. Chem Eng Science 2001;56:3931–49.
[2] Hlatky GG. Chem Rev 2000;100:1347–76.
[3] Xu R, Liu D, Wang S, Mao B. Macromol Chem Phys 2006;207:779–86.
[4] Nakayama Y, Saito J, Banko H, Fujita T. Chem Eur J 2006;12:7546–56.
[5] Severn JR, Chadwick JC. Macromol Rapid Comm 2004;25:1024–8.
[6] Severn JR, Chadwick JC. Macromolecules 2004;37:6258–9.
[7] Alobaidi F, Ye Z, Zhu S. Macromol Chem Phys 2003;204:1653–9.
[8] Choi Y, Soares JBP. Macromol Chem Phys 2009;210:1979–88.
[9] Preishuber-Pflugl P, Brookhart M. Macromolecules 2002;35:6074–6.
[10] Schrekker HS, Kotov V, Preishuber-Pflugl P, White P, Brookhart M. Macromolecules 2006;39:6341–54.
[11] Wilke G. Angew Chem Int Ed 1988;27:185–206.
[12] Schneider H, Puchta GT, Kaul FAR, Sieber GR, Lefebvre F, Saggio G, et al. J Mol Catal A: Chem 2001;170:127–41.
[13] Finch WC, Gillespie RD, Hedden D, Marks TJ. J Am Chem Soc 1990;112:6221–32.
[14] Gate DP, Svejda SA, Onate E, Killian CM, Johnson LK, White PS, et al. Macromolecules 2000;33:2320–34.
[15] Jamjah R, Zohuri GH, Javaheri M, Nekoomanesh M, Ahmadjo S, Farhadi A. Macromol Symp 2008;274:148–53.